Werk

Jahr: 1985
Kollektion: fid.geo
Signatur: 8 Z NAT 2148:57
Digitalisiert: Niedersächsische Staats- und Universitätsbibliothek Göttingen
Werk Id: PPN1015067948_0057
PURL: http://resolver.sub.uni-goettingen.de/purl?PPN1015067948_0057

LOG Id: LOG_0011
LOG Titel: Global seismic network assessment for teleseismic detection of underground nuclear explosions
LOG Typ: article

Übergeordnetes Werk

Werk Id: PPN1015067948
PURL: http://resolver.sub.uni-goettingen.de/purl?PPN1015067948
OPAC: http://opac.sub.uni-goettingen.de/DB=1/PPN?PPN=1015067948

Contact

Niedersächsische Staats- und Universitätsbibliothek Göttingen
Georg-August-Universität Göttingen
Platz der Göttinger Sieben 1
37073 Göttingen
Germany
Email: gdz@sub.uni-goettingen.de

J Geophys (1985) 57:1–13

Journal of Geophysics

Global seismic network assessment for teleseismic detection of underground nuclear explosions

I. Model calculations for different amplitude-attenuation curves

H.-P. Harjes
Geophysical Institute, Ruhr-University, D-4630 Bochum, Federal Republic of Germany

Abstract. The detection capability of a global seismic network is examined on the basis of a probability model. Given the location of seismograph stations with known background noise level, a worldwide grid of epicentres and amplitude-distance attenuation curves, the detection capability is expressed by the magnitude corresponding to a fixed probability that a specified minimum number of stations detect an event.

A globally distributed network – composed by an international group of seismologists (network III from CCD/558, 1978) – is selected as a model. These stations are judged to produce the best seismological results currently achievable for teleseismic detection. Multiwave detection criteria are applied which take variation of attenuation for different wave types into consideration. The extention of amplitude-attenuation curves to include core phases is investigated and effects of regional attenuation are studied. Depending on the detection criterion and attenuation curve, magnitude thresholds of a 50-station network can vary significantly.

Magnitude thresholds for this hypothetical network – requiring a 90% probability of at least four detecting stations – range from $3.4 \leqq m_b \leqq 3.6$ for Scandinavia and Europe, from $3.7 \leqq m_b \leqq 3.9$ for North America, Asia and Arctica, from $3.8 \leqq m_b \leqq 4.0$ for South America, Africa and Antarctica and $3.9 \leqq m_b \leqq 4.2$ for Australia, New Zealand and the Pacific.

Key words: Seismic detection probability – Magnitude threshold – Amplitude-attenuation curve – Global networks – Underground nuclear explosions

Introduction

"Although seismological capacity for identifying underground nuclear explosions may now be secondary to the political will of parties engaged in Comprehensive Test Ban negotiations it is still important to present the clearest possible evaluation of the role seismology might play should a Comprehensive Test Ban become reality."

This quotation from a 12-year-old paper (Marshall and Basham, 1972) is still an adequate description of the general purpose of studies on seismic verification of nuclear test ban treaties. In a more specific sense, we want to assess the detection threshold of a network of modern seismic stations. Detection thresholds will be given in terms of magnitude. Therefore, thresholds described herein apply to both shallow earthquakes and underground explosions without regard to source type. The important questions of source identification and yield estimation are not addressed in this paper.

Previous detection studies include the SIPRI-report (Davies, 1969), an analysis initiated by the United Nations (Basham and Witham, 1970) and a report of a group of seismologists to the Conference on Disarmament in Geneva (CCD/558, 1978). All of these assessments present conceptually similar schemes whereby worldwide existing seismological facilities are applied to a straightforward statistical estimation model. Given a globally distributed network of seismograph stations with known background noise level, a set of epicentre locations and standard amplitude-distance attenuation curves for seismic waves, the detection capability is expressed by the magnitude corresponding to a fixed probability that a specified minimum number of stations detect an event.

A second group of papers (Kelly and Lacoss, 1969; Report US/GSE/7, 1980) describe a different approach to examine the detection capability of a seismic network by including average worldwide seismicity. Using known earthquake recurrence rates, a synthetic list of events is produced as a reasonable approximation to those actually observed in a specific time interval. Keeping station parameters unchanged, this method allows an independent check on the results of studies of the first kind.

Finally, a third procedure starts from real data collected during special experiments (Lacoss et al., 1974) or published in bulletins by international agencies [e.g. International Seismological Centre (ISC) in Newbury, UK] and estimates detection thresholds with the use of Gaussian or maximum-likelihood techniques (Ringdal et al., 1977; Ringdal, 1984).

Estimates of the capabilities of seismic networks differ substantially as a result of these various approaches. In general the detection threshold increases in the order of the described procedures. Some reasons for these differences are obviously due to the difference between operational station performance used in the last approach and the idealized assumptions based on pure noise statistics which are input to the process

mentioned first. Smaller discrepancies simply reflect the difficulty in making this type of estimate and should be kept in mind in judging the accuracy of the results.

The main purposes of this study are:

i) To examine recently published approaches to network detection capability estimation by using multiwave detection criteria. A computer coded version of this procedure (Ciervo et al., 1983) was made available at the Center for Seismic Studies (CSS) in Arlington, VA. This code, called "Seismic Network Assessment Program for Detection (SNAPD)", not only models the propagation of P waves which were employed in previous programs (Wirth, 1977) but takes all relevant seismic phases into account and calculates wave attenuation and travel time as a function of regional media characteristics and event type.

ii) To study the influence of geophysical input parameters on the outcome. These parameters include, especially, the amplitude-attenuation curves at teleseismic distances and also the extension to core phases. Variations of attenuation in tectonic and stable areas at regional distances are of importance for detailed epicentre-station configurations. Special attention will be given to amplitude-attenuation curves derived from seismograms of underground nuclear explosions; otherwise earthquake data are included using shallow events.

Analysis of network detection probabilities

The statistical model and basic computational procedures are described in this section.

The model includes various parameters to be known at the beginning. The most important are
- Seismic station locations and their noise statistics (mean and variance)
- Amplitude-distance relations for several phases (besides P waves the prominent regional phases, Pg and Lg, are used)
- Signal variance
- Signal-to-noise ratio required for detection.

The procedure is then to do the following:
- Select a source location and compute detection probabilities for each station as a function of event magnitude.
- Find the lowest magnitude for which there is a defined probability to meet the specific detection criterion. (The most frequent criterion for global detection studies asks for a 90% probability of detecting P waves by at least four stations.)

First a single station is considered and the probability that it detects a certain wave is derived. Then the multiwave detection probability and the network capability are defined. We closely follow the notation by Ciervo et al. (1983). Further details can be found in Wirth (1977), Elvers (1980) and Evernden (1969a, b, 1975).

p_{ijk} denotes the probability that wave k propagated from epicentre j will be observed at station i. It is given by

$$p_{ijk} = R_i \Phi \left[\frac{\log A_{ijk}^{(\alpha)} - (\mu_{ik} + \log r_{ik})}{\sqrt{\sigma_{n_{ik}}^2 + \sigma_{s_{ik}}^2 + \sigma_{bk}^2}} \right], \tag{1}$$

where

$$\Phi(x) \equiv \int_{-\infty}^{x} e^{\frac{-y^2}{2}} \frac{dy}{\sqrt{2\pi}} \tag{2}$$

is the normal cumulative probability function.

In Eq. (1), signal and noise are assumed to be log-normally distributed (Freedman, 1967) and the log of the noise amplitude has expectation μ_n and variance σ_n^2, and the variance of the log of the signal is σ_s^2.

σ_{bk}^2 defines the additional variance of the log signal amplitude for wave k, given an m_b value; hence $\sigma_{bk} \equiv 0$ if k denotes the P wave. A station i is supposed to detect wave k provided that the ratio of signal to noise is at least r_{ik}.

Given an event at epicentre j of magnitude m_b and distance Δ_{ij} from station i, the amplitude of wave k at that station is calculated as

$$\log A_{ijk}^{(\alpha)} = m_{k_j} + b_k^{(\alpha)}(\Delta_{ij}) + c_k^{(\alpha)} \log(\Delta_{ij}) + \varepsilon_{ijk}, \tag{3}$$

for both stable ($\alpha = S$) and tectonic ($\alpha = T$) media.

For waves other than conventionally used P-phase, m_b has to be converted into an adequate magnitude m_k given the respective regression formula

$$m_k = [KE]_k + [KM]_k m_b. \tag{4}$$

The b_k and c_k in Eq. (3) are attenuation table entries and ε_{ijk} is the epicentre-station calibration term for wave k.

If wave k does not require regional attenuation or if $\Delta > 25°$ then $\log A_{ijk}$ is computed directly from Eq. (3) using a stable medium attenuation table. Otherwise, for regional distances ($\Delta \leqq 25°$)

$$\log A_{ijk} = (1 - w_{ij}) \log A_{ijk}^{(S)} + w_{ij} \log A_{ijk}^{(T)}, \tag{5}$$

where w_{ij} is the regional path weight; i.e. the ratio of the length of the wave path in tectonic media to the total great-circle path length Δ_{ij}. Especially if the epicentral path is assumed to have passed a region that severely attenuates Lg waves, then $\log A_{ij(lg)} = -\infty$.

If the attenuation table entries are δ_k, b_k, c_k, then, for $\delta_{k-1} < \Delta_{ij} < \delta_k$,

$$b_{\Delta_{ij}} \equiv b_k \quad \text{and} \quad c_{\Delta_{ij}} \equiv c_k \tag{6}$$

exept that if $c_k = 0$, linear interpolation is used for b:

$$b_{\Delta_{ij}} = b_k - (\delta_k - \Delta_{ij})[b_k - b_{k-1}]/(\delta_k - \delta_{k-1}). \tag{7}$$

The station's probability of detection p_{ijk}, given by Eq. (1), is influenced by the reliability R_i of its operation. p_{ijk} includes, therefore, a factor R_i, $0 < R_i \leqq 1$. R_i is of course dependent on a number of local circumstances which are not well known. Usually we set $R_i = 1$, assuming perfect operation.

Given the probability for a single station to detect an individual wave, we have to develop a procedure for multiwave network detection criteria that uses combinations of dependent wave arrivals at individual stations. An essential feature in the development of the model is the assumption that a minimum of four phases (not more than two of which are recorded at the same station) are required for detection assessment. Re-

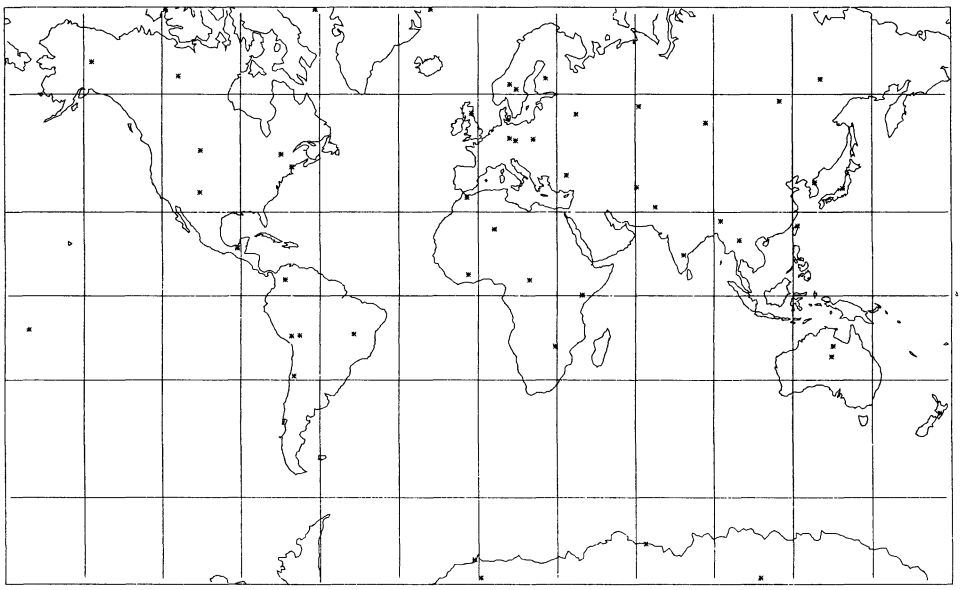

Fig. 1. Global seismic network (50 stations from CCD/558, 1978)

laxations of this requirement are possible and will be used when regional detection probabilities are estimated.

As an example, we illustrate the detection criterion

$$(Pg \cap Lg)/2 \cup P/4, \tag{8}$$

which literally means that a network detection consists of at least a two-station detection of Pg and Lg regional waves or at least a four-station detection of P waves or both. Expression (8) consists of two subcriteria

$$\boldsymbol{D}^1 = (Pg \cap Lg)/2, \qquad \boldsymbol{D}^2 = P/4$$

which specify different wave combinations.

Detection criteria such as Eq. (8) have to be decomposed and reduced to a set of canonical probabilities. Therefore, the logical expression (8) is transformed into an algebraic expression involving the marginal probabilities of independent subcriteria and the joint probabilities of dependent pairs of subcriteria. This transformation eliminates all logical "or" ($\cup$) among subcriteria by use of the elementary rule

$$\begin{aligned}\text{prob}[\boldsymbol{D}^1/n \cup \boldsymbol{D}^2/m] = \text{prob}[\boldsymbol{D}^1/n] + \text{prob}[\boldsymbol{D}^2/m] \\ - \text{prob}[\boldsymbol{D}^1/n \cap \boldsymbol{D}^2/m],\end{aligned} \tag{9}$$

where, if $\boldsymbol{D}^1$ and $\boldsymbol{D}^2$ are independent wave criteria

$$\text{prob}[\boldsymbol{D}^1/n \cap \boldsymbol{D}^2/m] = \text{prob}[\boldsymbol{D}^1/n]\,\text{prob}[\boldsymbol{D}^2/m]. \tag{10}$$

In the case of Eq. (10), independent calculations for each individual wave define the probability $\text{prob}[\boldsymbol{D}^1_{(n':N)}]$ that exactly n' out of N stations detect wave combination $\boldsymbol{D}^1$. If, however, the detection subcriteria $\boldsymbol{D}^1$ and $\boldsymbol{D}^2$ have waves in common, like

$$(Lg/2 \cap P/1) \cup P/4,$$

then computation of the joint probability, Eq. (10), does not split into independent probabilities.

Clearly the probability $\text{prob}[\boldsymbol{D}^1/n]$ of at least n detecting stations follows as:

$$\text{prob}[\boldsymbol{D}^1/n] = \sum_{n'=n}^{N} \text{prob}[\boldsymbol{D}^1_{(n':N)}]. \tag{11}$$

Thus we need only compute the probability of exactly n' detecting stations.

In a concluding step, a binary search is used to find the magnitude value that results in p_t, the threshold probability for network detection.

Let m_i be a sequence of test magnitudes $m_{\min} \leqq m_i \leqq m_{\max}$ such that each m_i results in a network detection probability p_i. Initially $m_1 = m_{\min}$. If $p_1 \geqq p_t$, the search is terminated; otherwise $m_2 = m_{\max}$ and if $p_2 \leqq p_t$, the search is also terminated.

Assuming $p_1 < p_t < p_2$,

$$m_i = (m_{i-1} + m')/2, \qquad i = 1, 2, 3, \ldots$$

where, if p_{i-1} is less than p_t, m' is the last test magnitude for which the corresponding network probability is greater than p_t, and vice versa. The search is continued until $i = i^*$ is reached such that

$$|p_{i^*} - p_t| \leqq \varepsilon,$$

corresponding to a threshold magnitude m_{i^*}.

Detection capability of a global network

In selecting a network for detection of seismic events based upon existing seismograph stations, it is desirable to

– arrive at a relatively uniform geographical distribution of stations

– select stations with modern instrumentation and optimum detection capabilities.

With these criteria in mind, a selection of relatively few stations is considerably more effective than using all (about 1,000) stations that routinely report to one of

Table 1. Stations used in network detection capability computations with noise statistics (mean and standard deviation of logarithms in nm) from CCD/558 (1978)

Station code	LAT $+=N$	Long $+=E$	SP-noise	
			Mean	STD
AFI	−13.91	−171.78	1.60	0.50
ALE	82.48	−62.40	0.70	0.40
ANMO	34.93	−106.45	0.30	0.20
ANTO	39.92	32.82	0.30	0.20
ARE	−16.46	−71.49	0.85	0.45
ASP	−23.68	133.90	0.48	0.30
BDF	−15.39	−47.54	0.48	0.30
BNG	4.37	18.57	0.00	0.15
BOCO	4.62	−74.07	0.30	0.20
BOD	57.85	114.18	0.70	0.40
BUL	−20.14	28.61	0.60	0.35
CMT	18.79	−98.98	0.30	0.20
COL	64.90	−147.78	0.70	0.40
COM	16.15	−92.07	1.40	0.50
DAG	76.77	−18.77	1.08	0.50
EKA	55.33	−3.16	0.90	0.45
ELT	53.25	86.27	0.70	0.40
GAC	45.70	−75.48	0.30	0.20
GBA	13.60	77.40	1.18	0.50
GRF	49.69	11.21	0.30	0.20
HFS	60.13	13.70	0.00	0.15
IFR	33.31	−5.07	0.90	0.45
JYS	62.17	24.87	0.30	0.20
KHC	49.13	13.58	0.48	0.30
KIC	6.36	−4.74	0.48	0.30
KSR	38.00	128.00	0.48	0.30
LAO	46.68	−106.22	−0.40	0.15
MAIO	36.31	59.59	0.30	0.20
MAT	36.54	138.21	1.00	0.50
MAW	−67.60	62.88	1.00	0.50
MBC	76.24	−119.36	0.78	0.45
NAO	61.04	11.22	−0.10	0.14
NIE	49.41	20.31	0.70	0.40
NIK	−1.27	36.80	0.30	0.20
OBN	55.17	36.60	0.78	0.45
PNS	−16.27	−68.47	0.48	0.30
QUE	30.18	66.95	1.00	0.50
SBA	−77.85	166.76	1.48	0.50
SHL	25.57	91.88	0.30	0.20
SNA	−70.32	−2.33	1.20	0.50
SPA	−89.90	0.10	0.90	0.45
SVE	56.80	60.63	0.78	0.45
TAM	22.79	5.52	0.60	0.35
TATO	25.03	121.52	0.60	0.35
TLL	−30.10	−70.48	1.08	0.50
WEL	−41.29	174.78	1.48	0.50
WES	42.38	−71.32	1.18	0.50
WRA	−19.95	134.35	0.30	0.20
YAK	62.02	129.72	0.70	0.40
YKA	62.49	−114.60	0.48	0.30

the international data centres. In a previous report (CCD/558, 1978) a network of 50 stations was composed which was judged to produce the best seismological results currently achievable for teleseismic detection of seismic events.

These stations, whose geographical distribution is shown in Fig. 1 and whose coordinates and further parameters are given in Table 1, are used as a reference network in our study. The global station distribution is not as uniform as desirable, having 36 stations in the northern hemisphere compared to 14 stations in the southern hemisphere or 31 stations in the eastern hemisphere compared to 19 in the western hemisphere, but it reflects to some extent the distribution of land masses on earth.

Mean value and standard deviation of logarithmic station noise which are used to calculate station detection probabilities from Eq. (1) are also included in Table 1 (columns 4 and 5). Due to the quoted report (CCD/558, 1978), average noise levels were partly derived from published noise power spectra, partly estimated from magnification curves of seismographs. Because of lack of adequate measurements, an adhoc procedure was used to estimate the variance of the station noise: those stations with higher noise level were also assigned greater variance.

As can be seen from Eq. (1), it is the combined effect of variance in noise amplitude and signal amplitude which influences the station detection threshold: it decreases as the denominator in Eq. (1) is increased, provided that the detection probability is less than 0.5, and vice versa. For the network, the detection threshold generally decreases when signal or noise variance is increased. For the 50-station network – introduced in Fig. 1 and Table 1 – a constant value for the standard deviation of signal amplitude (0.2 in logarithmic units) was used. Test runs showed that doubling this parameter to 0.4 result in a very small difference of the network detection threshold (not exceeding 0.1 magnitude unit). Consequently, network capability is not very sensitive to this parameter.

There are two other input parameters to Eq. (1) which are to be assumed in an adhoc manner: the reliability factor R describing grossly the station operation (up-time), is set in our calculations to 1.0. Earlier studies (Ringdal et al., 1977) have estimated this parameter to range from 0.8 to 1.0 for most of the stations selected for our network.

A minimum signal-to-noise ratio has to be chosen to detect seismic signals emerging from background noise. Throughout this study a s/n ratio [r_{ik} in Eq. (1)] of 1.5 was chosen. The capability results are easily transformed to correspond to other s/n ratios, since this parameter occurs as a difference $(m-\log r_{ik})$ in Eq. (1). Thus a simple relationship exists between the chosen value of r_{ik} and the corresponding magnitude level. If r_{ik} is increased from 1.5 to 3.0, for example, the threshold will be increased by $(\log 3-\log 1.5)=0.3$ magnitude units.

Amplitude-attenuation curves at teleseismic distances: $25° < \Delta < 100°$

Several investigations of amplitude attenuation with distance have been made since the pioneering work of Gutenberg and Richter (1956). Following their paper, we will summarize amplitude-distance relations from Eq. (3) in the form

$$B(\Delta)=b(\Delta)+c\cdot\log(\Delta).$$

So we can interpret B values in terms of magnitude units.

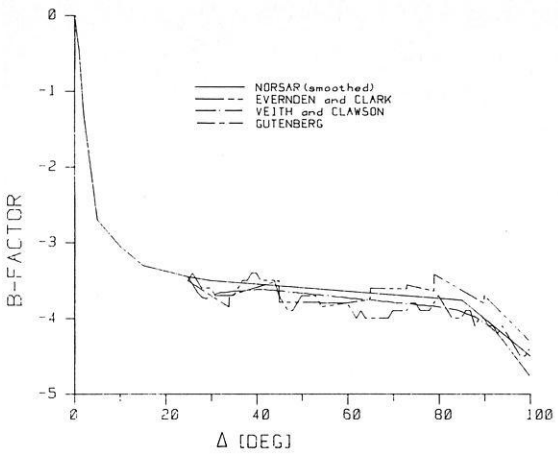

Fig. 2. Teleseismic attenuation curves for *P*-wave amplitudes

In Fig. 2, the results of Evernden and Clark (1970), Veith and Clawson (1972) and NORSAR (Ringdal and Fyen, 1979) are compared to the Gutenberg and Richter curve. Whereas Everden and Clark and Veith and Clawson use mostly explosions and a station network of mainly LRSM-stations in the US, the Ringdal-Fyen curve is derived from ISC bulletin data (1971–1976) of 136 globally distributed WWSSN stations.

All curves have been arbitrarily connected at regional distances to focus upon the differences in the teleseismic window. The principal difference between Veith-Clawson and NORSAR curves on the one hand and Gutenberg-Richter and Evernden-Clark curves on the other hand appears in the fact that the former indicate smooth amplitude variations from mantle discontinuities, whereas the latter indicate several stepwise changes in amplitude as a function of distance.

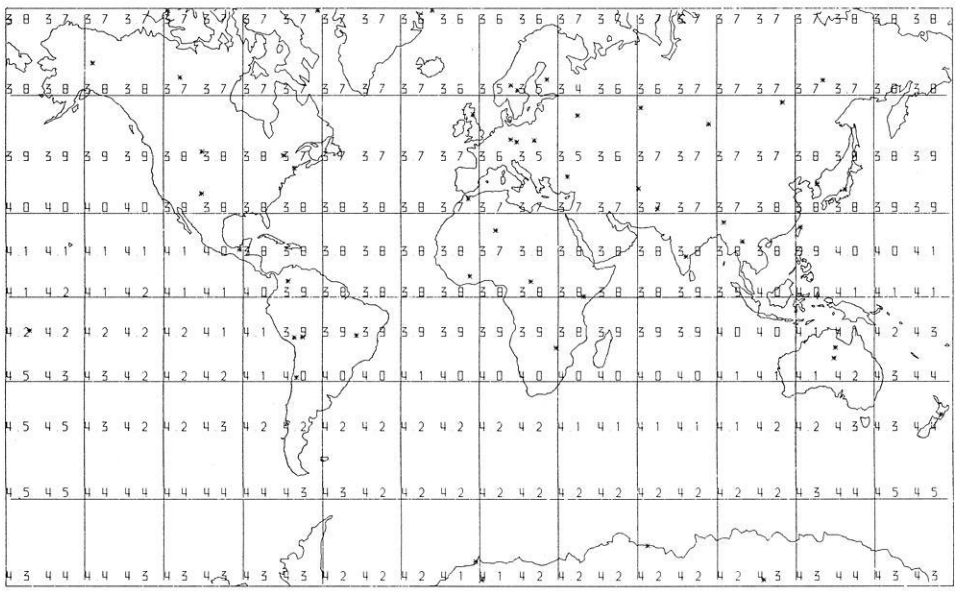

Fig. 3. 50-station network detection capability corresponding to a 90% probability of (at least) 4 detecting stations. NORSAR attenuation curve is used

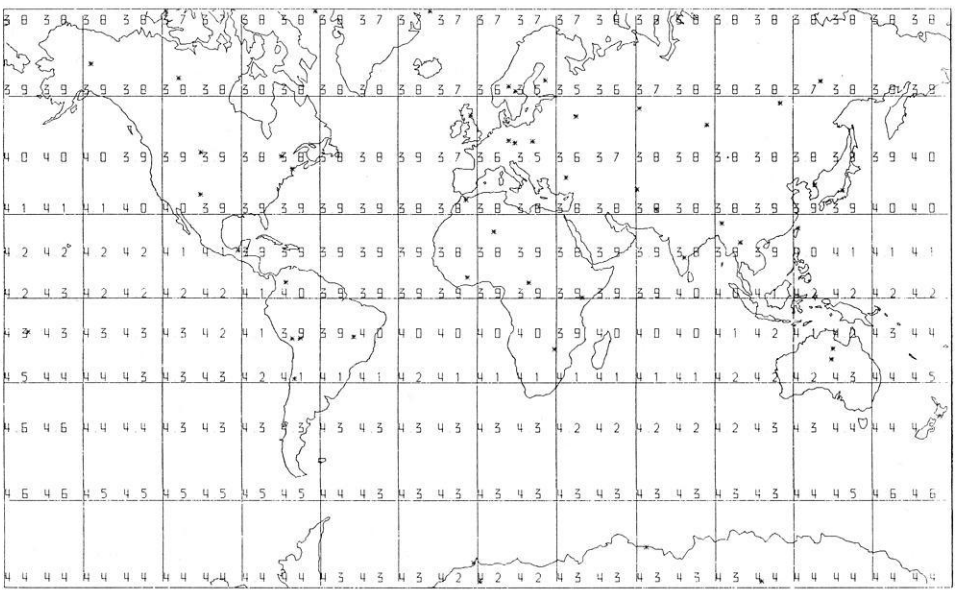

Fig. 4. 50-station network detection capability using Veith and Clawson attenuation curve. Other parameters are the same as in Fig. 3

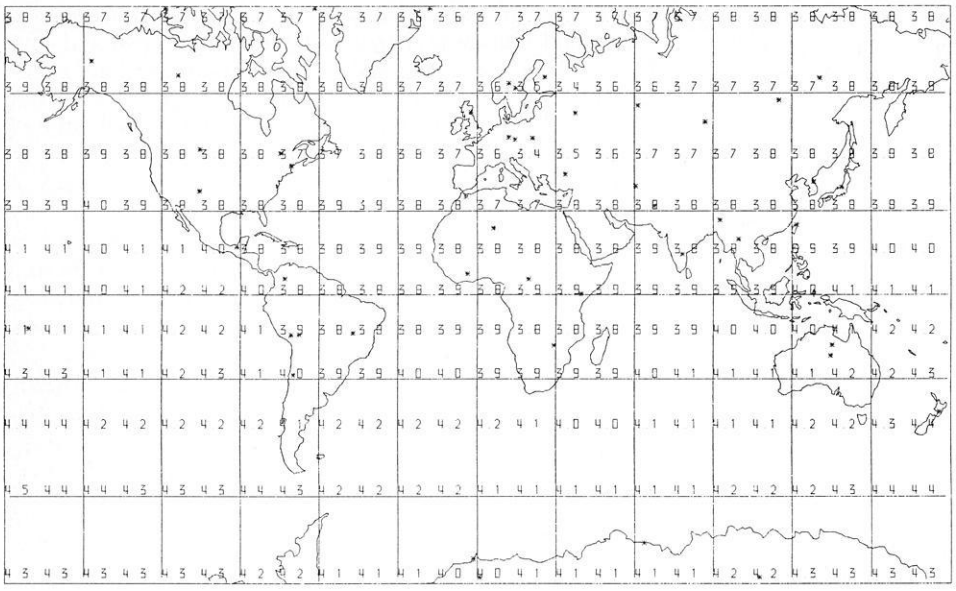

Fig. 5. 50-station network detection capability using Evernden and Clark attenuation curve. Other parameters are the same as in Fig. 3

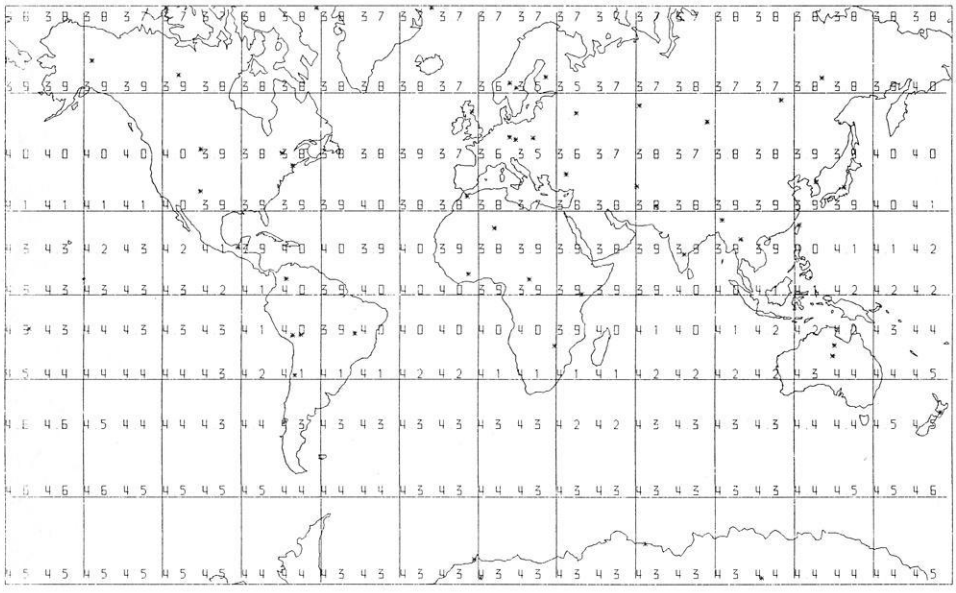

Fig. 6. 50-station network detection capability using Gutenberg and Richter attenuation curve. Other parameters are the same as in Fig. 3

The general difference between Veith-Clawson and Norsar attenuation curves is nearly a constant 0.1 magnitude unit over the whole teleseismic range. This may result from the fact that the Veith-Clawson curve was corrected for surface focus events; and the NORSAR curve, in comparison, comprises measurements from shallow earthquakes. Additionally, we have smoothed the minimum at 30° distance for NORSAR data. The obvious distinction between the curves of Gutenberg-Richter and Evernden-Clark appears in the far teleseismic portion where a difference of 0.3 magnitude units can be found. This is a consequence of the way Evernden and Clark have chosen to normalize their data.

Some of these differences can be seen in the network detection capability which is shown in Figs. 3–6. Using a 15° epicentre grid, the 90% probability of at least four detecting stations was calculated. For the NORSAR attenuation function (Fig. 3), which will be used as a reference curve in this study, the magnitude threshold is estimated to be from m_b 3.4–3.7 in Europe and Scandinavia, m_b 3.7–3.8 in North America, Asia and Arctica, m_b 3.7–4.0 in Africa and most parts of South America, whereas we get values up to $m_b = 4.5$ in the Pacific region. The slight difference between the eastern and western hemisphere (about 0.2 magnitude units) as well as the large difference of more than one magnitude unit between the northern and southern hemisphere mainly result from the station distribution of the network. The high station noise at the sites in the Pacific (New Zealand and Samoa) gives an additional contribution to the low detection capability in the southern hemisphere.

As expected from the preceding discussion of attenuation curves (Fig. 2), detection thresholds for the network increase globally by about 0.1 magnitude units using the Veith-Clawson data. The Evernden-Clark curve has a remarkable effect in lowering the detection

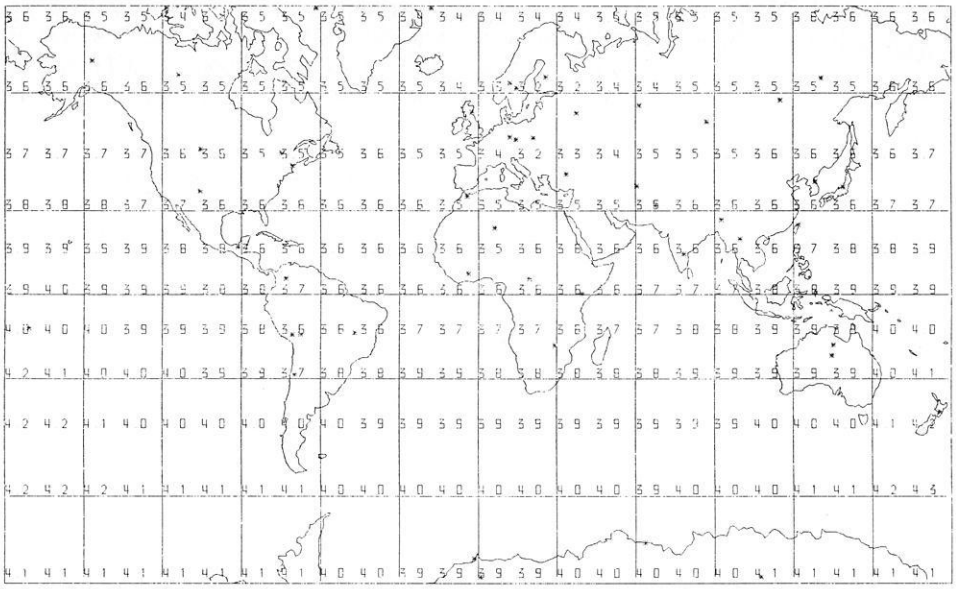

Fig. 7. 50-station network detection capability for 30% probability of 4 detecting stations. NORSAR attenuation curve is used

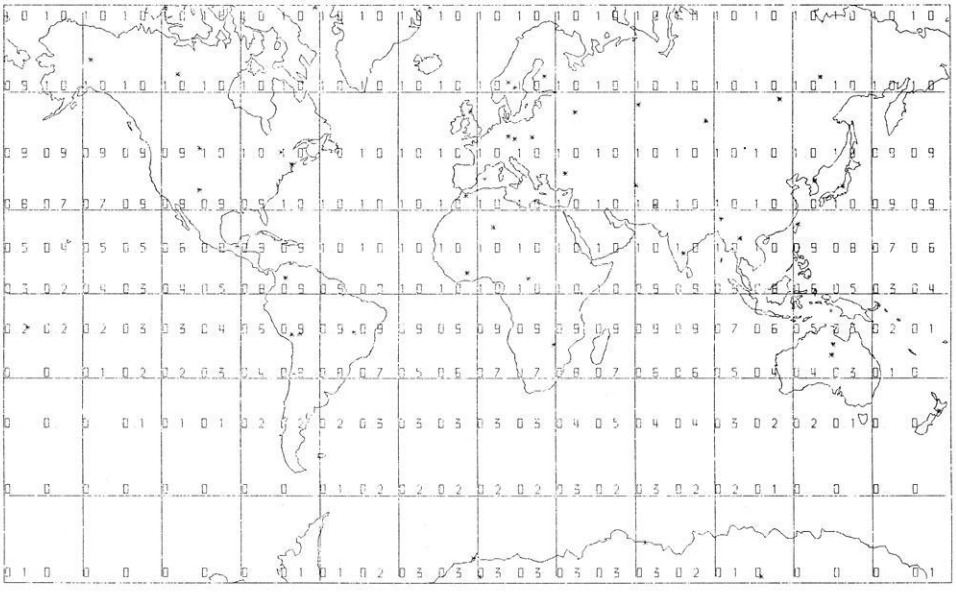

Fig. 8. 50-station network detection probability at fixed magnitude $m_b = 4$. NORSAR attenuation curve is used

threshold in the southern hemisphere by about 0.3 magnitude units (Fig. 5), again not unexpected from the shape of the attenuation curve which shows pronounced lower B values at far teleseismic distances than any other attenuation curve in Fig. 2. Finally, the Gutenberg-Richter curve yields detection thresholds (Fig. 6) very similar to the Veith-Clawson curve (Fig. 4).

We can conclude from these calculations that stepwise changes or fluctuations in the attenuation curve do not significantly affect the global detection capability of a 50-station network. Of course these discontinuities have remarkable focussing-defocussing effects for specific epicentre-station configurations, but these are smoothed and can not be resolved by global grids of 15° size. These peculiarities are better implemented by use of epicentre-station calibration factors expressed by ε_{ijk} in Eq. (3).

For all computations we kept the probability level at 90%. In changing this parameter one can significantly influence detection thresholds (of course the seismological capability is not changed at all). At the 30% probability level (Fig. 7) we get 0.2–0.4 magnitude units lower thresholds compared to the commonly accepted 90% probability level.

Another way of demonstrating this difference is to calculate the network detection probability for a fixed magnitude value. Figure 8 shows the global distribution of probabilities to detect a magnitude 4 event. Besides Antarctica, New Zealand, the Pacific islands and the tip of South America, the chance of detecting events on land down to this size at (at least) four stations is higher than 80%.

Extension of amplitude-attenuation curves beyond 100° distance

The most prominent result of the last section is the clear difference in detection capability between the north-

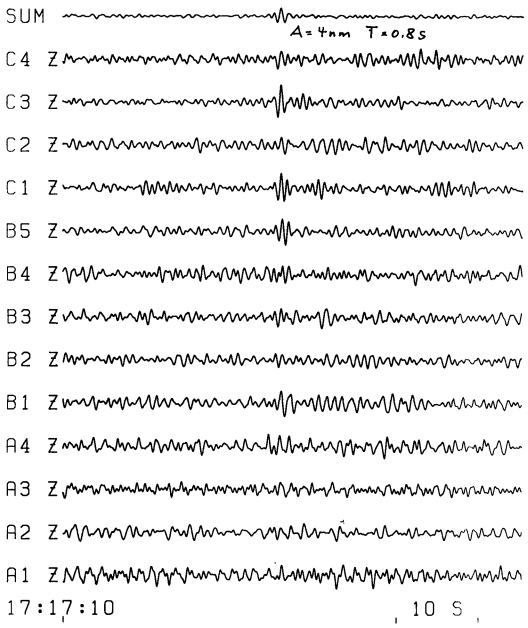

Fig. 9. French nuclear test recorded with Graefenberg array seismometers. Distance to test site is 143.7°. Amplitude on summation trace is 4 nm at 0.8 s

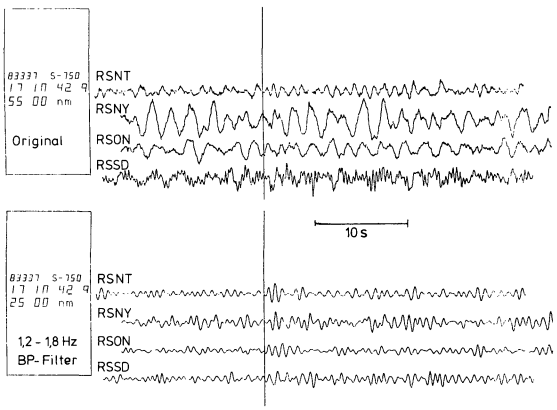

Fig. 10. RSTN-recordings of French nuclear test from previous figure. *Upper traces* are original data, *lower traces* are bandpass-filtered

ern and southern hemisphere regardless of what type of attenuation function was applied in the teleseismic window. To reduce the detection threshold in the southern hemisphere, a substantial increase in the number of stations in that region has often been recommended. Although this is a solution in principle, there are several practical problems with its realization. The major part of the southern hemisphere is covered by deep ocean areas where installation and maintenance of seismographs is still difficult and expensive. Islands are known for a high microseismic noise level and poor detection capability.

An attractive alternative for improving the detection capability in the southern hemisphere is provided by the use of signals which have travelled through the earth's core and are routinely detected at stations beyond 100° distance. In a specific window, i.e. $142° < \Delta < 152°$, these refracted core phases offer even better detection possibilities than earlier described direct *P* waves. Numerous studies have shown that observation of high amplitudes for various *PKP* branches can be a powerful tool in lowering detection thresholds (Blandford and Sweetser, 1973; Quamar, 1973). This can easily be demonstrated with a seismogram of a French nuclear underground explosion exploded at Mururoa atoll (21 S, 140 W) and recorded with the Graefenberg array in Germany ($\Delta = 143.7°$). Figure 9 shows a recording at all 13 vertical elements of the array (for a more detailed description, see Harjes and Seidl, 1978) and the beam-trace on top from which a displacement amplitude of 4 nm at a period of 0.8 s was measured.

In comparison, Fig. 10 shows recordings of the same event by the RSTN-stations in North America. These stations (Engdahl et al., 1982) are new borehole installations and include seismometers (Geotech S-750) with high sensitivity in the short-period band. Traces are aligned to the theoretical arrival time of the *P* wave which is marked by the cursor line. The stations have a distance of 73°–88° from the event. Neither the original (upper part) nor the narrow-band filtered (lower part) traces meet the detection requirement set in our calculations. Correspondingly, this event was not reported by international data centres, which restrict their event-defining association process to *P* arrivals within 100° distance.

Table 2 shows the summary of station reportings for this event available from GTS/WMO-channels at the CSS. The association program implemented at the CSS found the questionable event by using *PKP* observations from three stations in Europe (including GRF). With the detection criterion we applied in the preceding paragraph (at least four *P* detections), this event would have been missed. Consequently, we amended amplitude-distance curves beyond 100° as shown in Fig. 11. There are two curves from different sources (Blandford and Sweetser, 1973; Ringdal, personal communication, 1984) which show a great similarity, although Blandford and Sweetser's curve is based on a

Table 2. Association result for French explosion using all WMO-messages at CSS

12/3/1983	OT = 16:58:3, 5	LAT = −20.95	LON = −139.87	H = 9 km	Tuamotu archipel	
Station	Arrival time	Phase	δt [sec]	Δ [Deg]	AMP [nm]	*T* [sec]
ALQ	17:8:38.0	P	−1.4	64.0	3.4	0.9
CTA	17:9:8.0	P	−0.5	68.6		
YKA	17:10:44.5	P	1.4	85.5	3.8	0.8
GRF	17:17:36.1	PKPAB	−0.3	143.3	4.0	0.8
PRU	17:17:39.0	PKPDF	0.3	144.7		
KHC	17:17:39.5	PKPDF	0.5	144.8		

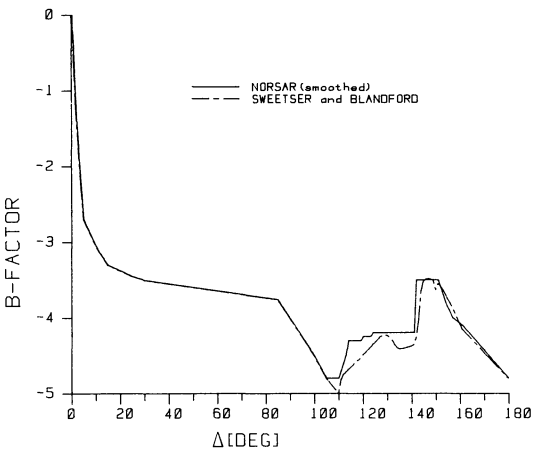

Fig. 11. Extension of amplitude-attenuation curve beyond 100° using *PKP* phases

more general data base (ISC) than Ringdal's data which are in use at the NORSAR array.

Detection threshold estimates for the 50-station network calculated with these attenuation curves differ less than 0.1 magnitude units. Israelson (1984) recommended the requirement of at least one *P* detection in addition to *PKP* arrivals to define an event to avoid large location errors because the stations observing *PKP* might be clustered in a narrow geographical area. Figure 12 gives the network detection capability for detecting at least four *P* or *PKP* arrivals, one of which has to be a direct *P* wave i.e. observed at a station within less than 100° distance of the event. This result can directly be compared with Fig. 3 because the attenuation functions are identical up to 100° distance.

The inclusion of *PKP* phases yields a large decrease of the detection threshold for the southern hemisphere (0.3–0.5 magnitude units) and divides the difference in detection capability between northern and southern hemispheres by half compared to the use of only *P* arrivals within 100° distance.

Variation of amplitude-attenuation curves at regional distances

In discussing the influence of varying teleseismic attenuation functions on the network detection capability, we always used the same curve for regional distances ($\Delta < 25°$).

Although the teleseismic part (including *PKP*) will be most important for a global network, regional differences will have some effect in areas (Europe and Scandinavia) where the 50-station network is highly represented. These areas give us the opportunity to study the effect of different regional attenuation functions which, in a gross sense, represent "stable" (i.e. high Q) and "tectonic" (i.e. low Q) provinces.

The distinction was initially introduced for the North American continent, taking into account the different crustal structure in western and eastern US (Evernden, 1967). In this section we discuss only the influence of variations of P_n wave which is seen as the first arrival on regional seismograms recorded at distances greater than 1°. To emphasize the difference, rather extreme representatives of published attenuation curves have been used, namely Evernden's "8.5" curve (Evernden, 1967) derived from data in the eastern US, $b = -0.83$, $c = -2$ in Eq. (3), compared to a P_n-attenuation curve derived from data in southwestern US (Der et al., 1982) which yield $b = 0.134$ and $c = -3.803$. Thus the main difference between these two types of regional attenuation curves is that the "stable" P_n drops off as the square of the distance, while the "tectonic" curve decreases more rapidly, almost with the fourth power of the distance.

Another peculiarity at regional distances is the relative maximum in the amplitude-distance curve as a result of the 20° discontinuity which is observed worldwide with differing prominence (Gutenberg and Richter, 1956; Veith and Clawson, 1972). To emphasize also the effect of the 20° discontinuity the Veith-Clawson curve has been appended to Evernden's curve in the distance range $17° < \Delta < 25°$. On the opposite side,

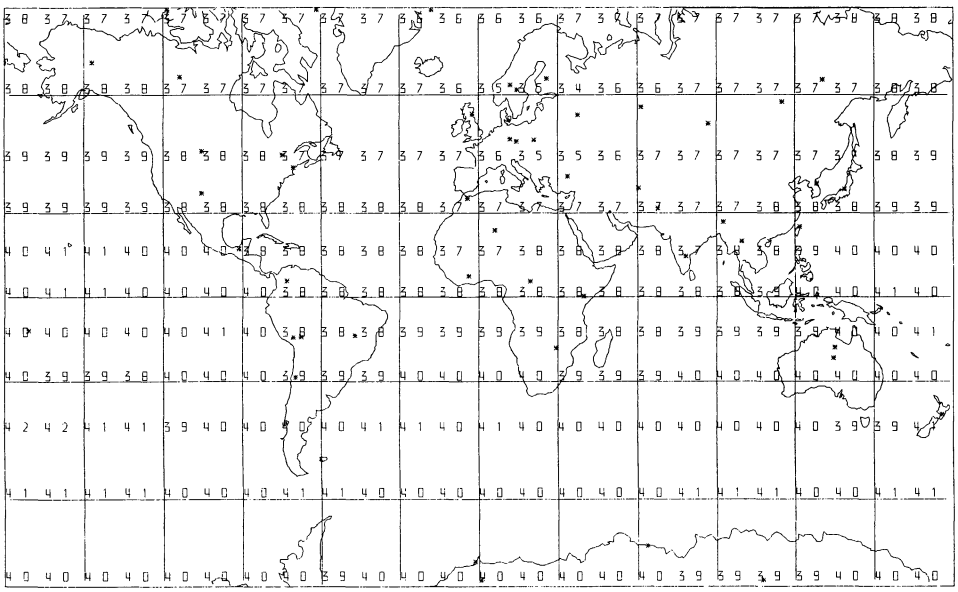

Fig. 12. 50-station network capability for (at least) 4 (*P* or *PKP*) detections. At least 1 station has to detect *P*. Other parameters are the same as in Fig. 3

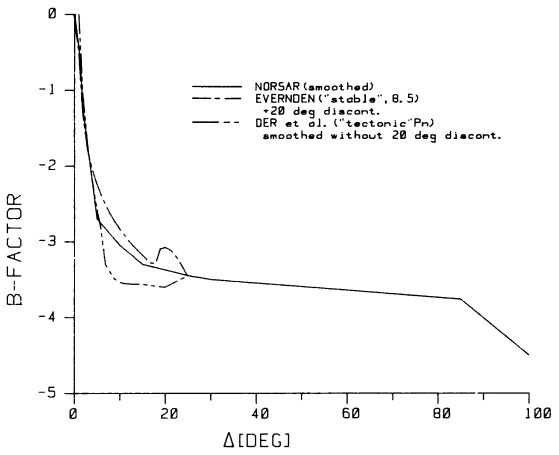

Fig. 13. Regional variation of attenuation curves to model "stable" and "tectonic" crustal wave paths

the "tectonic" attenuation curve has been smoothly connected to teleseismic distances without consideration of a 20° discontinuity.

Our final regional extensions of attenuation functions are plotted in Fig. 13. It is again noted that these curves are artificial compositions to show the most pronounced effect on network detection capability. The result can be seen in Figs. 14 and 15 which are to be compared to Fig. 12. Using specified regional attenuation curves generally increases the influence of station distribution. Global differences of detection thresholds are pronounced in Fig. 14, which shows the influence of a "stable" (Evernden "8.5"+20° disc) regional attenuation curve. At close-to-station distances, detection thresholds are decreased by up to 0.2 magnitude units as compared to Fig. 12. On the contrary, detection thresholds are increased for most parts of Eurasia and America by up to 0.2 magnitude units for a "tectonic" attenuation curve (Fig. 15). Worldwide, this attenuation curve smooths the difference in detection capability between northern and southern hemispheres; certainly a result of our station distribution.

In summary, regional variations of *P*-wave amplitude-attenuation curves can change the detection threshold of a global 50-station network by as much as ± 0.2 magnitude units.

Regional detection probabilities of a global network

Although this paper mainly deals with teleseismic detection capabilities, it is interesting to investigate to what extent the magnitude threshold of a global network will be influenced by including phases other than P_n phases. It should be mentioned at the beginning that this section is intended as an amendment to teleseismic capabilities. To study the full potential of regional waves for detection purposes a regional station network has to be introduced. This is beyond the scope of this report and for details on this matter we refer to excellent recent review articles (Pomeroy et al., 1982; Blandford, 1981).

It is well known that the largest amplitudes on a short-period regional seismogram occur within the *Lg* wavetrain which may be interpreted as a superposition of a large number of higher mode Love and Rayleigh waves – *Lg* amplitudes can be 10 times larger than the maximum amplitude of the first arrival (*P* wave) at the same distance and in the same period band around 1 s. The actual amplitude can drastically vary due to local geology. An extensive literature exists on amplitude-distance attenuation curves for *Lg* for various regions of the world (for reference, see the above-mentioned review articles).

Again we extract two extreme representatives of published curves to examine the effect on the detection capability. As representing "stable" regions with low attenuation, we choose an attenuation curve published by Nuttli (1973). Nuttli derived an amplitude decay with distance proportional to $\Delta^{-5/3}(0.5° < \Delta < 40°)$ corresponding to the shape of the well-known "Prague"-formula (Vanek et al., 1962) adopted by IASPEI to be used for teleseismic Rayleigh wave observations. However, Nuttli derived his curve from observations of 1 s

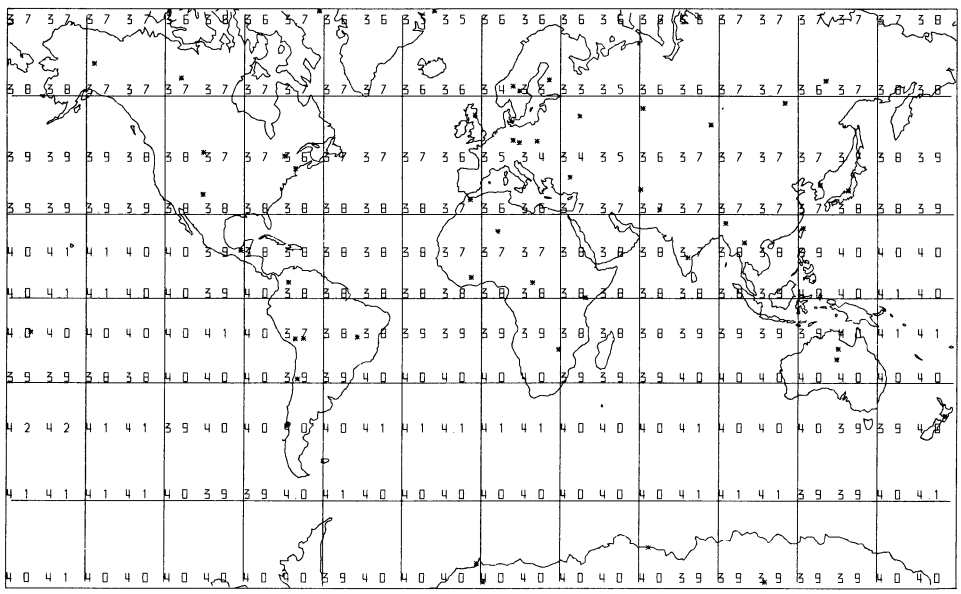

Fig. 14. 50-station network detection capability using "stable" attenuation curve from Fig. 14. Other parameters are the same as in Fig. 3

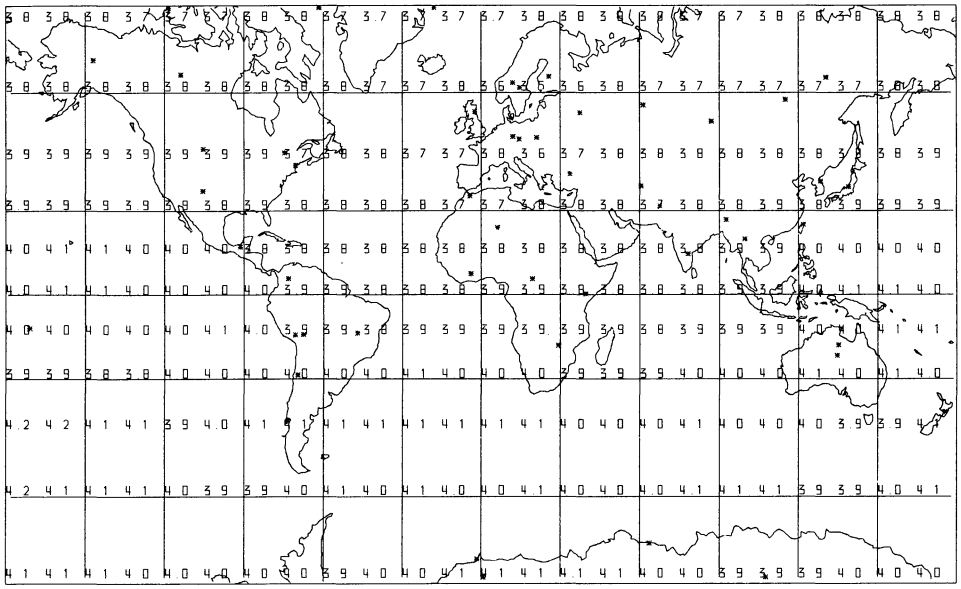

Fig. 15. 50-station network detection capability using "tectonic" curve from Fig. 14. Other parameters are the same as in Fig. 3

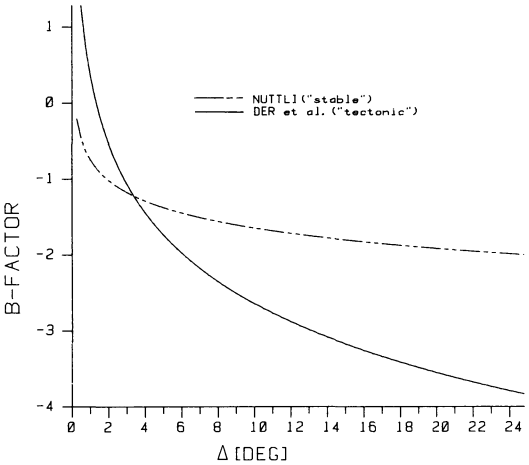

Fig. 16. Amplitude attenuation curves for *Lg* waves in "stable" and "tectonic" areas

Lg waves in the eastern US, whereas the "Prague"-formula is valid for Raleigh waves around 20 s.

For crustal structures in "tectonic" provinces like the western US, an amplitude-distance decay for *Lg* proportional to Δ^{-3} was observed (Der et al., 1982). The selected attenuation curves are plotted in Fig. 16. In estimating detection capabilities by use of *Lg* waves it has to be mentioned that its amplitude not only varies regionally but it can also be totally suppressed. Representing a wave guide phenomenon, *Lg* propagation is seriously affected by variations in crustal thickness (mountains, ocean-continent and/or tectonic boundaries). To take these inefficient wavepaths into account a much finer grid than the $15° \times 15°$ grid used in our calculations has to be applied.

We want to examine whether inclusion of *Lg* waves has an effect on a global network at all. If there appear regional improvements of the detection capability, these have to be verified by considering the corresponding regional crustal structure. Because we want to insist on teleseismic detections we use *Lg* detections only if at least one station of the network observed a teleseismic *P* wave ($\Delta > 25°$). So we required at least two *Lg* detections and one teleseismic *P* detection or four *P* detections. As *Lg* is observed on all three components of ground motion, an azimuth estimate can be calculated and two stations are sufficient to roughly associate the event origin. An event is declared if at least one *P* observation at teleseismic distances confirms this association.

Figures 17 and 18 show the detection capability using this criterion for Nuttli's and Der et al.'s attenuation function, respectively. In comparison to Figs. 14 and 15, which show the corresponding *P*-wave detection results, thresholds are lowered by 0.1–0.3 magnitude units. Again it should be emphasized that these improvements are irrelevant if they occur in oceanic areas because *Lg* waves disappear after crossing approximately 100 km of oceanic structure. Restricting the evaluation to continental areas only, it can be seen from Figs. 17 and 18 that the detection threshold is mostly influenced in the southern hemisphere where occasionally two stations are located at regional distances. In Europe and Scandinavia we already reach a high capability for four *P* detections which is not significantly improved by the additional (two *Lg* and one teleseismic) detection probability.

Finally, it might be mentioned that the detection difference caused by the difference of the two attenuation curves (Fig. 16) is only marginal for the selected detection criteria and station spacing of our global network.

Conclusions

Estimation techniques to examine seismic network detection capabilities, including multiwave criteria, are well established. For the hypothetical 50-station network studied in this report, best estimates of magnitude thresholds requiring a 90% probability of at least four detecting stations range from

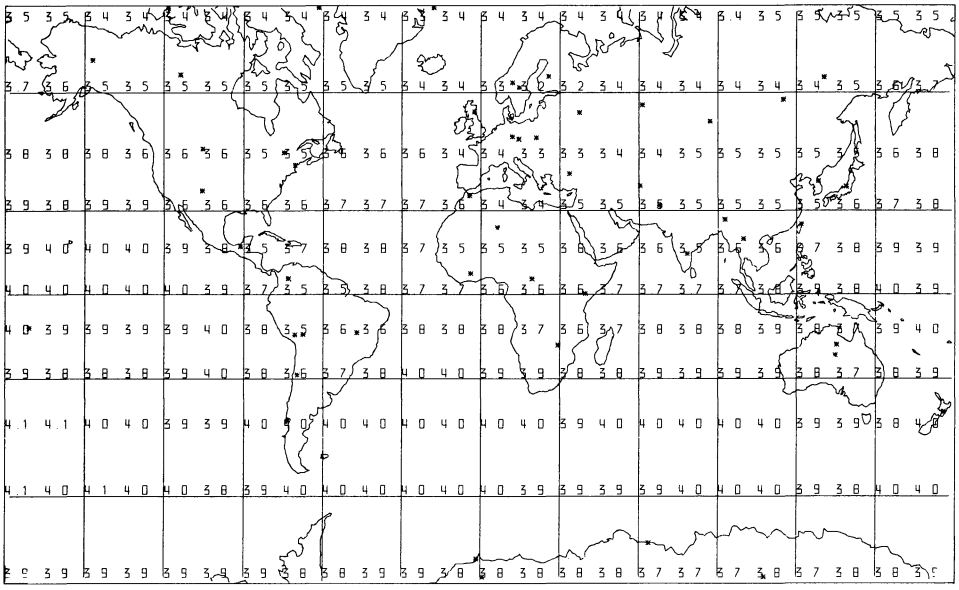

Fig. 17. 50-station network capability to detect (at least) *Lg* waves at 2 stations and *P* waves at 1 station or *P* waves at 4 stations. "Stable" attenuation curve for *Lg* waves is used

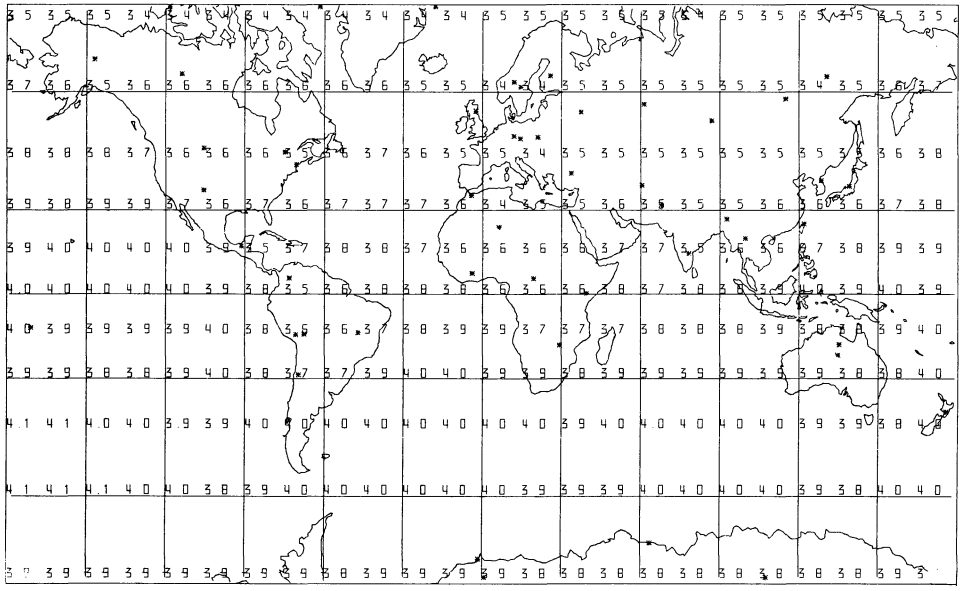

Fig. 18. 50-station network capability to detect (at least) *Lg* waves at 2 stations and *P* waves at 1 station or *P* waves at 4 stations. "Tectonic" attenuation curve for *Lg* waves is used

$3.4 \leqq m_b \leqq 3.6$ for Scandinavia and Europe,
$3.7 \leqq m_b \leqq 3.9$ for North America, Asia and Arctica,
$3.8 \leqq m_b \leqq 4.0$ for South America, Africa and Antarctica,
$3.9 \leqq m_b \leqq 4.2$ for Australia, New Zealand and the Pacific.

Of course it has to be kept in mind that the results are based upon the particular input values chosen. In this report we have mainly studied the influence of different amplitude-attenuation curves and various wave types on the detection threshold of a global network. The essential conclusion from our calculations is a strong recommendation to extend the *P*-wave attenuation curves to *PKP* phases. This yields a large decrease of the detection threshold for the southern hemisphere and will reduce the difference in present detection capabilities between northern and southern hemispheres.

Emphasis is stressed upon teleseismic capabilities, regional effects are limited by the station spacing within our network. Varying some input parameters, e.g. signal-to-noise ratio or station reliability, the estimates of detection threshold can easily be re-evaluated; the influence of others, e.g. signal variance or detection probability, can generally be estimated without reference to the specific configuration of the network.

Certainly, estimates of detection thresholds strongly depend on station locations and their noise statistics. As a starting model we have restricted our calculations to the hypothetical network composed by the Geneva group (CCD/558, 1978). In a subsequent paper we will compare these results with actual station reportings from a 2month data exchange experiment which included noise measurements. For the first time these data will allow the derivation of noise statistics on a global scale for simultaneously reported seismic events.

Acknowledgements. This work was carried out during a visit to the Center for Seismic Studies (CSS) in Rosslyn, Virginia.

The author is especially indebted to R. Alewine and A. Kerr from the U.S. Defense Advanced Research Projects Agency for their kind invitation. The support of C.F. Romney and the entire staff at the CSS is gratefully acknowledged. Many of the ideas in this paper resulted directly or indirectly from discussions with F. Ringdal to whom the author is deeply indepted. He further wishes to thank R. Suey, Pacific-Sierra Research, for his support in making SNAP/D run at the CSS, and W.J. Hannon, Lawrence Livermore Laboratory, for a critical review of the manuscript.

References

Basham, P.W., Whitham, K.: Seismological detection and identification of underground nuclear explosions. Report, EPB, Department of Energy, Mines and Resources, Ottawa, Canada, 1970

Blandford, R.R.: Seismic discrimination problems at regional distances. NATO, Advanced Study Institutes, Series C, 74. Dordrecht, Holland: D. Reidel Publ. Comp., 1981

Blandford, R.R., Sweetser, E.I.: Seismic distance-amplitude relations for short period *P*, *P*diff, *PP* and compressional core phases for delta >90 deg. Report, Teledyne-Geotech, SDAC-TR-73-9, Alexandria, VA, 1973

CCD/558: Report to the Conference of the Committee on Disarmament of the Ad Hoc Group of Scientific Experts to Consider International Cooperative Measures to Detect and to Identify Seismic Events. Geneva, Switzerland, 1978

Ciervo, A.P., Sanemitsu, S.K., Snead, D.E., Suey, R.W.: Seismic network assessment program for detection. Report 1027A, Pacific-Sierra Research, Los Angeles, CA, 1983

Davies, D. (Rapporteur): Seismic methods for monitoring underground explosions. SIPRI, Stockholm, Sweden, 1969

Der, Z.A., O'Donnell, A., McElfresh, T.W., Julita, R., Burnetti, J.A., Marshall, M., Silk, M., Gordon, E.: A study of seismic wave propagation at regional distances in five areas of the world. Report, Teledyne-Geotech, VSC-TR-82-14, Alexandria, VA, 1982

Elvers, E.: The capability of a network of seismological stations to detect events and to obtain identification parameters. Report, FOA, C 20231-T1, Stockholm, Sweden, 1980

Engdahl, E.R., Peterson, J., Orsini, N.A.: Global digital networks – Current status and future directions. Bull. Seismol. Soc. Am. **72B**, S243–S260, 1982

Evernden, J.F.: Magnitude determination at regional and near-regional distances. Bull. Seismol. Soc. Am. **57**, 591–639, 1967

Evernden, J.F.: Precision of epicentres located by small numbers of worldwide stations. Bull. Seismol. Soc. Am. **59**, 1365–1398, 1969a

Evernden, J.F.: Identification of earthquakes and explosions by use of teleseismic data. J. Geophys. Res. **74**, 3828–3856, 1969b

Evernden, J.F.: Further studies on seismic discrimination. Bull Seismol. Soc. Am. **65**, 359–392, 1975

Evernden, J.F., Clark, D.M.: Study of teleseismic *P*. II.-Amplitude data. Phys. Earth Planet. Int. **4**, 24–31, 1970

Freedman, H.: Estimating earthquake magnitude. Bull. Seismol. Soc. Am. **57**, 747–760, 1967

Gutenberg, B., Richter, C.F.: Magnitude and energy of earthquakes. Ann. Geofis. **9**, 1–15, 1956

Harjes, H.-P., Seidl, D.: Digital recording and analysis of broad-band seismic data at the Graefenberg (GRF)-array. J. Geophys. **44**, 511–521, 1978

Israelson, H.: Experiments with a computer program for automatic association of seismic events. Unpublished Manuscript, 1984

Kelly, E.J., Lacoss, R.T.: Estimation of seismicity and network detection capability. Technical Note 1969–41, Lincoln Lab, MIT, Mass., 1969

Lacoss, R.T., Needham, R.E., Julian, B.R.: International seismic month event list. Technical Note 1974-14, Lincoln Lab., MIT, Mass., 1974

Marshall, P.D., Basham, P.W.: Discrimination between earthquake and underground explosions employing an improved Ms scale. Geophys. J. R. Astron. Soc. **28**, 431–458, 1972

Nuttli, O.W.: Seismic wave attenuation and magnitude relations for eastern North America. J. Geophys. Res. **78**, 876–885, 1973

Pomeroy, P.W., Best, W.J., McEvilly, T.V.: Test ban treaty verification with regional data – A review. Bull. Seismol. Soc. Am. **72B**, S89–130, 1982

Quamar, A.: Revised velocities in the Earth's core. Bull. Seismol. Soc. Am. **63**, 1073–1105, 1973

Ringdal, F.: Study of magnitudes, seismicity and earthquake detectibility using a global network. NORSAR Semiann. Techn. Summ., Kjeller, Norway, 1984

Ringdal, F., Fyen, J.: Analysis of global *P*-wave attenuation characteristics using ISC data files. NORSAR Semiann. Techn. Summ., Kjeller, Norway, 1979

Ringdal, F., Huseby, E.S., Fyen, J.: Earthquake detectibility estimates for 478 globally distributed seismograph stations. Phys. Earth Planet. Int. **15**, 24–32, 1977

US/GSE/7: Investigation of the properties of CD-network III using synthetic data. Report of the United States Delegation, Geneva, Switzerland, 1980

Vanek, J.A., Zatopek, V., Karnik, N.V., Kondorskaya, Y.V., Rizinichenko, E.F., Savarenski, E.L., Solov'ev Shebalin, N.V.: Standardization of magnitude scales. Bull. (Izvest.) Acad. Sci. USSR, Geophys. Ser. **3**, 108, 1962

Veith, K.F., Clawson, G.E.: Magnitude from short-period *P*-wave data. Bull. Seismol. Soc. Am. **62**, 435–452, 1972

Wirth, M.H.: Estimation of network detection and location capability. Report, Teledyne-Geotech, Alexandria, VA, 1977

Received October 18, 1984; Revised Version February 21, 1985
Accepted February 25, 1985